NATIONAL ADVISORY COMMITTEE FOR AERONAUTICS

TECHNICAL NOTE 3123

EFFECT OF VARIOUS ARRANGEMENTS OF TRIANGULAR LEDGES ON THE PERFORMANCE OF A 23° CONICAL DIFFUSER AT SUBSONIC MACH NUMBERS

By Jerome Persh and Bruce M. Bailey

Langley Aeronautical Laboratory
Langley Field, Va.

Washington
January 1954

NATIONAL ADVISORY COMMITTEE FOR AERONAUTICS

TECHNICAL NOTE 3123

EFFECT OF VARIOUS ARRANGEMENTS OF TRIANGULAR LEDGES ON THE PERFORMANCE OF A 23° CONICAL DIFFUSER AT SUBSONIC MACH NUMBERS

By Jerome Persh and Bruce M. Bailey

SUMMARY

A brief investigation has been made to determine whether the use of annular ledges to promote turbulent momentum exchange will improve the performance of a short, wide-angle diffuser. Results are presented of tests of a 23° conical diffuser with a 2:1 ratio of exit to inlet area with both rough and smooth triangular ledges, approximately one-tenth of the inlet boundary-layer thickness in height, installed in succession from the inlet to the exit. The results show that, although the flow in the diffuser without ledges was very unstable, the presence of a roughness strip near the inlet, with or without additional ledges, assured stable flow. For the configurations investigated, the static-pressure recovery and the total-pressure-loss coefficient were either unaffected or only slightly impaired by the installation of the ledges.

INTRODUCTION

Because of space limitations in present-day aircraft, considerable effort has been directed toward improving the performance characteristics of short, wide-angle diffusers. Substantial improvements in the static-pressure recovery of short diffusers may be achieved by using devices such as vortex generators which accelerate the turbulent exchange of momentum. From indications of the literature (refs. 1 to 3), ledges placed on the diffuser wall transverse to the direction of flow might also serve as a means for accelerating the turbulent exchange of momentum and, consequently, be used to improve the performance of short diffusers.

The results of several previous experimental investigations (refs. 1 to 3) indicate that the velocity profile measured in the region downstream of a ledge on a flat plate had a shape that was an improvement over velocity profiles measured on the same surface at the same points in the absence of the ledge. In references 1 and 2 the separated boundary layer leaving the trailing edge of the ledge is shown experimentally to reattach

violently to the surface several ledge heights downstream, and the intensities of the longitudinal fluctuations in the boundary layer in this region are much greater than those found on the corresponding smooth surface. The increased momentum transfer downstream of the ledge exerts a strongly favorable influence on the shape of the boundary-layer velocity profile and this influence persists for a distance of approximately 200 ledge heights in the direction of flow. Moreover, this favorable effect on the shape of the velocity profile was found to exist for flows with adverse pressure gradients.

A brief program was organized to investigate the effects of a series of ledges on the performance of a short, wide-angle diffuser. The over-all effect on the diffuser performance was the principal consideration, and no effort was expended to determine the boundary-layer behavior in the immediate vicinity of the ledge. For the systematic installation of various combinations of both rough and smooth ledges, the over-all performance characteristics of a 23° conical diffuser with a 2:1 ratio of exit to inlet area were determined in order to explore the potential of this device. The height of most ledges was approximately one-tenth of the inlet boundary-layer thickness.

SYMBOLS

D	diameter
p	static pressure
h	total pressure
q_c	impact pressure
M	Mach number
W	weight flow
T	stagnation temperature, °R
P	barometric pressure, in. Hg
ρ	mass density
$\Delta\bar{h}$	weighted total-pressure loss from surveys
L	diffuser length
r	radial distance from center line

R	radius
Re	Reynolds number based on inlet diameter, $\rho \frac{UD}{\mu}$
x	distance along longitudinal axis
y	perpendicular distance from diffuser wall
u	local velocity at any point in airstream
U	velocity of stream outside boundary layer
$\frac{u}{U}$	velocity ratio $\left(\text{for incompressible flow, } \sqrt{\frac{h - p}{h_{max} - p}}\right)$
δ	boundary-layer thickness at $u/U = 0.95$
δ^*	boundary-layer displacement thickness for incompressible flow, $\delta \int_0^1 \left(1 - \frac{u}{U}\right) d \frac{y}{\delta}$
θ	boundary-layer momentum thickness for incompressible flow, $\delta \int_0^1 \frac{u}{U}\left(1 - \frac{u}{U}\right) d \frac{y}{\delta}$
μ	viscosity
H	boundary-layer shape parameter, δ^*/θ

Diffuser performance parameters:

$\frac{\Delta \bar{h}}{q_{c_1}}$	total-pressure-loss coefficient
$\frac{\Delta p}{\Delta p_{ideal}}$	diffuser effectiveness

Subscripts:

0	reference conditions
1	conditions at diffuser inlet
2	conditions at diffuser exit
3	conditions at tailpipe exit
a	actual measured quantity
s	referred to standard conditions
max	maximum value

APPARATUS AND METHODS

Test Setup

A schematic drawing of the duct system used for this investigation is shown in figure 1. The test duct system consists of a 23° conical diffuser with a 2:1 ratio of exit to inlet area joined to a 21-inch-diameter cylindrical approach tube approximately $4\frac{1}{2}$ inlet diameters in length. The junction between the approach tube and diffuser was formed as a circular arc of $5\frac{3}{16}$-inch radius, tangent to both the inlet cylinder and the diffuser cone. A discharge tailpipe of 29.75-inch diameter, approximately $3\frac{1}{2}$ inlet diameters in length, was attached to the diffuser exit. Prior to initial ledge tests, the diffuser was tested without ledges in order to provide data for comparison purposes. For all ledge tests, a 1-inch-wide strip of roughness, identified as ledge a, was installed near the diffuser inlet to stabilize the flow, as shown in figure 2.

Description of Ledges

All ledges, both rough and smooth, were 1 inch wide. The rough ledges were made of graded cork particles that would pass through a standard screen with 8 meshes to the inch, but be retained on a screen with 14 meshes to the inch; the average height of the particles used was 0.10 inch. The height of most ledges was approximately one-tenth of the inlet boundary-layer thickness.

The following procedure was used to install a typical rough ledge:

(1) A band of cork particles, 1 inch wide, was cemented to the diffuser wall, transverse to the direction of flow, in the proper axial location.

(2) The leading edge was buffed and faired to give the strip an approximately triangular cross section with a trailing edge about 0.10 inch high. A view of the approximate cross section of some typical rough ledges appears in figure 2.

The smooth ledges were made of balsa-wood strips of triangular cross section which were installed in the diffuser in such a manner as to have the leading edge smoothly faired into the diffuser wall. After installation, each balsa-wood strip was carefully filled and sanded to produce a smooth ledge surface.

The axial position and alphabetical designation of the ledges are shown in figure 1. Configuration a has a single 1-inch-wide, 0.1-inch-high roughness strip, designated ledge a, installed near the diffuser inlet (see fig. 1). The first ledge and each succeeding ledge was installed as indicated in figure 1. Each configuration tested is identified by a letter which denotes the position of the last ledge installed for that configuration. The following table gives a description of all the ledge configurations investigated:

Configuration	Number of rough ledges	Height, in.	Number of smooth ledges	Height, in.
a	1	0.10	---	----
b	2	.10	---	----
b-1	1	.10	1	0.10
b-2	1	.10	1	.15
b-3	1	.10	1	.20
c	3	.10	---	----
d	4	.10	---	----
d-1	{1	.10	---	----
	{3	.20	---	----
d-2	1	.10	3	.10
e	5	.10	---	----
f	6	.10	---	----
g	7	.10	---	----

Instrumentation and Calibration

A series of static-pressure orifices was installed along a single generatrix running from the diffuser inlet to the tailpipe station in order to measure longitudinal static-pressure distributions. At stations 1, 2, and 3 (the diffuser inlet, diffuser exit, and tailpipe exit, respectively), wall-static-pressure measurements were made at six equally spaced circumferential positions. All static-pressure orifices were connected to a multitube manometer and pressures were recorded photographically. Total- and static-pressure stream surveys were made at stations 2 and 1, in that order, for all the ledge configurations by using three equally spaced, remotely controlled, electrically driven pressure probes. A sketch of a pressure probe is included in figure 1.

The flow conditions at the diffuser inlet were determined by making pressure-probe surveys at three equally distributed positions around the circumference of the inlet. The diffuser inlet calibration is shown in figure 3, in which the inlet Mach number, the Reynolds number based on inlet diameter, and the weight flow adjusted for standard conditions of 29.92 inches of mercury and 60° F are all plotted as functions of the inlet pressure ratio p_1/p_0. Typical velocity profiles at the inlet station 1 are shown in figure 4 for several values of p_1/p_0. The inlet boundary-layer thickness was of the order of 5 percent of the inlet diameter.

Accuracy of Measurements

For some of the configurations investigated, the occurrence of separation or asymmetrical flows or the presence of turbulent fluctuating velocities cast doubt on the accuracy of the results obtained. Comparisons between inlet and exit weight-flow values, shown for all configurations, give some indication of the inaccuracy resulting from these effects.

CALCULATION OF PERFORMANCE PARAMETERS

The reference static pressure p_0 used in conjunction with the inlet static pressure p_1 provided the required correlating parameter for calculating all performance characteristics.

The volume-weighted mean loss in total pressure from the reference station 0 to the station under consideration was computed in the following manner:

$$\overline{(p_0 - h_x)} = \frac{\int_0^R u(p_0 - h_x) r \, dr}{\int_0^R ur \, dr} \tag{1}$$

The loss in mean total pressure was computed for the diffuser by using the equation

$$\Delta\bar{h}_{1,2} = \overline{(p_0 - h_2)} - \overline{(p_0 - h_1)} \tag{2}$$

in which the inlet pressure ratio p_1/p_0 is used as a correlating parameter. If expressed nondimensionally by dividing by the impact pressure of the inlet, the parameter $\Delta\bar{h}/q_{c_1}$ can be defined as the total-pressure-loss coefficient.

The rise in static pressure was computed as the difference between the arithmetic mean of the six wall-static-pressure measurements at station 1 and the arithmetic mean of the wall-static-pressure measurements at station 2 or 3. The ideal static-pressure difference was determined by assuming frictionless one-dimensional incompressible flow for the same values of p_1/p_0. The ratio of the measured static-pressure rise to the ideal difference $\Delta p/\Delta p_{ideal}$ is defined as the diffuser effectiveness.

RESULTS AND DISCUSSION

In contrast to the flow in the diffuser with no ledges, which periodically shifted position and lacked axial symmetry, the flow in the diffuser with one or more ledges installed was steady and, in general, had approximately symmetrical velocity profiles at the diffuser exit for most configurations. Because the flow was so unstable in the diffuser without the inlet roughness strip, ledge a, accurate total-pressure measurements could not be made at the diffuser exit. Therefore, in order to provide values of $\Delta\bar{h}/q_{c_1}$ for comparison purposes, total-pressure surveys were made at station 3 where the flow was steady. In subsequent sections, comparisons are made between the values of $\Delta\bar{h}/q_{c_1}$ measured at station 3 for the diffuser with no ledges and the values of $\Delta\bar{h}/q_{c_1}$ measured at station 2 for the ledge configurations. These comparisons give a

convenient index of the relative effect of various ledge arrangements on the total-pressure-loss coefficient. It should be noted that all values of $\Delta\bar{h}/q_{c_1}$ given for the diffuser without ledges include the total-pressure loss occurring in the tailpipe, and all values of $\Delta\bar{h}/q_{c_1}$ given for the ledge configurations are for the diffuser alone. Values of the diffuser effectiveness for the diffuser with and without ledges are compared at both the diffuser exit and the tailpipe exit.

Rough Ledges

Diffuser effectiveness.- The variation of $\Delta p/\Delta p_{ideal}$ with inlet pressure ratio at the diffuser exit, station 2, and at the tailpipe exit, station 3, is shown in figure 5 for all configurations except the single-ledge case for which data at station 3 are unavailable. For comparison purposes, the curves of diffuser effectiveness for the no-ledge configuration have been added. In general, values of diffuser effectiveness at the diffuser exit for all ledge configurations are less than those for the diffuser without ledges. At the tailpipe exit, station 3, this difference between results for ledge and no-ledge configurations (for ledge configurations b, c, d, and g) is less than that found at the diffuser exit. For configurations e and f, values of diffuser effectiveness measured at the tailpipe exit are slightly higher at lower speeds than the values for the diffuser without ledges.

Total-pressure-loss coefficient.- The variation in $\Delta\bar{h}_{1,2}/q_{c_1}$ with inlet pressure ratio is illustrated in figure 6 for ledge configurations a, b, c, d, f, and g. Because of a faulty pressure tube, the results obtained for ledge configuration e are considered unreliable and are not presented. For purposes of comparison, the curve of $\Delta\bar{h}_{1,3}/q_{c_1}$ for the diffuser without ledges, measured at the tailpipe exit, station 3, is included in figure 6. It should be noted that, in general, the differences between the values of total-pressure-loss coefficient for the diffuser with and without ledges apparently becomes larger for successive configurations b, c, and d. These differences diminish, however, for ledge configuration f and become imperceptible for configuration g at a value of p_1/p_0 of about 0.95. Because of asymmetrical flow conditions which were found to exist for configurations f and g, the values of total-pressure-loss coefficient shown in figures 6(e) and (f), however, are not considered accurate.

Summary of performance results.- Figure 7(a) shows the variation of $\Delta p/\Delta p_{ideal}$ with the position of x/L corresponding to the number of

ledges installed, at stations 2 and 3 for a constant inlet pressure ratio of 0.95; the ratio x/L is defined as that portion of the diffuser length over which the ledges were installed. At the diffuser exit, as the number of ledges installed was increased, the diffuser effectiveness decreased progressively until, with seven ledges installed, a decrease in the effectiveness of about 7 percent was obtained. At the tailpipe exit the effect of the ledges was also detrimental, but on the order of a maximum of 2 percent. The net effect on the diffuser effectiveness of the ledge installations indicates, therefore, that the ledges were not effective diffuser boundary-layer control devices.

Figure 7(b) demonstrates the variation of $\Delta\bar{h}_{1,2}/q_{c_1}$ with the position of x/L corresponding to the number of ledges installed at a constant inlet pressure ratio of 0.95. The curves of figure 7 indicate that the over-all effect of the ledges on the diffuser performance was relatively small. The static-pressure recovery characteristics were diminished for all ledge configurations and the total-pressure-loss coefficients were diminished for most of the ledge configurations. These curves appear to represent some inconsistency in the results. Inconsistencies are also evident in figure 8, in which the weight flows are plotted as functions of the inlet pressure ratio for ledge configurations b, c, d, f, and g. The computed weight flows at the diffuser exit are seen to be larger than the inlet weight flows for configurations b, c, and d over the entire speed range. As pointed out in reference 4, this condition is an anticipated result for boundary-layer flows such as those encountered in this experiment. As noted previously, asymmetrical flow conditions existed at the diffuser exit for configurations f and g, and this occurrence is probably responsible for the discrepancies observed between the computed values of W_s at the diffuser exit and the inlet weight flows.

Apparent discrepancies of the nature of those found for configurations b, c, and d have been traced to the influence of turbulent fluctuating velocities on the total-pressure measurements (ref. 4). In this reference a method for estimating the effect of such fluctuating velocities on diffuser-performance calculations has been devised. The procedure presented therein has been applied to the data of the present investigation for configurations b, c, and d. The results of this analysis are shown in figures 6 and 7. Apparently, the trend of the curve of computed values of $\Delta\bar{h}_{1,2}/q_{c_1}$ against x/L plotted in figure 7(b) is compatible with the trend of the diffuser effectiveness curve of figure 7(a), and a progressive diminution of performance with number of ledges installed is indicated. This result substantiates the conclusion relative to the diffuser effectiveness, which is that the ledge installations were not effective diffuser boundary-layer control devices.

Boundary-layer velocity profiles at diffuser exit.- Boundary-layer velocity profiles computed from total-pressure measurements made at station 2 are shown in figure 9 for configurations b, c, d, f, and g. The boundary-layer parameters δ^*, θ, and H given for each of the profiles presented were computed by using definitions for two-dimensional flow uncorrected for compressibility effects. It should be noted that evidence of separated flow was found for all configurations shown with the exception of configuration b. For configurations b, c, and d, the separated regions, where detected, were very small, and symmetrical flow conditions were observed. Violent oscillations of the fluid in the manometer tubes, usually characteristic of separated flow, were not observed and the data were repeatable in all cases. The boundary-layer velocity profiles for all configurations are of interest with regard to the high values of boundary-layer shape parameter obtained. Over the range of configurations the values of H vary from about 3.2 to 4.6, which is above the normal range for steady flow in smooth-wall diffusers. The separated-flow regions and the high values of shape parameter are further evidence that the ledge installations did not perform as anticipated. An interesting observation is that the values of H for configurations b, c, and d are of the order of 3.5, whereas the values of H for configurations f and g are of the order of 4.5. This occurrence is probably attributable to the onset of asymmetrical flow conditions and the proximity of the probe to the trailing edge of the ledges.

Longitudinal static-pressure distributions.- The variation in static pressure along the wall of the diffuser is shown in figure 10 for a typical ledge configuration for a number of different speeds identified by the value of p_x/p_0 at $x = 0$. Static-pressure distributions for each of the ledge configurations are not presented because no significant differences could be detected. In the vicinity of the initial ledge the static-pressure measurements are erratic, apparently because of the presence of the ledge and the high boundary-layer velocity close to the wall. Downstream of this point, however, the ledges do not appear to have influenced the static-pressure measurements, which would tend to indicate that the downstream ledges were ineffective in promoting the diffusion.

The validity of the wall-static-pressure measurements in the neighborhood of the ledges was verified by stream survey-tube measurements in the same regions.

Effect of ledge height.- In order to determine whether favorable results could be achieved by the use of higher rough ledges, the rough ledges b, c, and d were constructed of cork particles so that the trailing edge was 0.20 inch high and the leading edge faired into the diffuser wall. This configuration is designated as configuration d-1.

Figures 11(a) and (b) show the variation of total-pressure-loss coefficient and diffuser effectiveness, respectively, with the inlet

pressure ratio for configuration d-1. For purposes of comparison, the curves for $\Delta\bar{h}_{1,2}/q_{c_1}$ and $\Delta p/\Delta p_{ideal}$ against p_1/p_0 for configuration d and values of $\Delta\bar{h}_{1,3}/q_{c_1}$ for the diffuser without ledges are included in figure 11. A check of the measured weight flows at the diffuser exit with the inlet flow calibration (see fig. 11(c)) indicated that the loss coefficient measurements for the dissimilar-ledge configuration required no corrections. A comparison of the experimental values of $\Delta\bar{h}_{1,2}/q_{c_1}$ for configuration d-1 and the calculated values of $\Delta\bar{h}_{1,2}/q_{c_1}$ for configuration d with the experimental values of $\Delta\bar{h}_{1,3}/q_{c_1}$ for the diffuser without ledges shows that, although no improvement in total-pressure performance over that for the diffuser without ledges was achieved through the use of higher rough ledges, the values of $\Delta\bar{h}_{1,2}/q_{c_1}$ are less for configuration d-1 than the corrected values for configuration d.

The values of $\Delta\bar{h}_{1,2}/q_{c_1}$ shown in figure 11(a) for configuration d-1 appear to be more or less constant over the speed range at approximately the same value as $\Delta\bar{h}_{1,3}/q_{c_1}$ for the diffuser with no ledges. However, the values of $\Delta p/\Delta p_{ideal}$ at both the diffuser exit and the tailpipe exit rise smoothly with increasing speed from a value considerably less than that for either configuration d or the diffuser with no ledges to values which are nearly the same as those for the diffuser without ledges. In fact, at the highest velocity points, the values of $\Delta p/\Delta p_{ideal}$ measured at the tailpipe exit for configuration d-1 are slightly greater that those for the diffuser with no ledges.

Comparison Between Smooth and Rough Ledges

In order to determine whether the performance characteristics measured with the four 0.10-inch rough ledges are duplicated by the use of geometrically similar 0.10-inch smooth ledges, three 0.10-inch balsa-wood ledges were installed in the diffuser downstream of the original 0.10-inch inlet rough ledge at the axial locations indicated in figure 1 for configuration d. The resulting configuration is designated as d-2. The variation of $\Delta p/\Delta p_{ideal}$ and $\Delta\bar{h}_{1,2}/q_{c_1}$ with p_1/p_0 is shown in figure 12 for configuration d-2. Also shown in figure 12 is a comparison between the performance results of configurations d and d-2.

The measured weight flows at the exit for configuration d-2 are shown by figure 12(c) to agree with the inlet measurements much more

closely than those for configuration d. The deviations obtained were not considered large enough to warrant correcting the loss coefficients.

From inspection of figure 12, the smooth ledges are seen to cause a deterioration of diffuser performance at the lower speeds. As the speed is increased, however, the values of $\Delta p/\Delta p_{ideal}$ rise smoothly while the values of $\Delta \bar{h}_{1,2}/q_{c_1}$ drop continuously. At the highest test speeds the diffuser effectiveness approaches asymptotically that of the rough-ledge case and the loss coefficient approaches that of the diffuser without ledges. Of the configurations tested, configuration d-2 exhibited the most favorable speed effects on the performance and, at the higher speeds, it produced better performance than the comparable rough-ledge case.

Effect of Changing Height of Smooth Ledge b

The variation of the diffuser performance with the height of the second ledge was determined by varying the height of ledge b from 0.10 inch to 0.20 inch in increments of 0.05 inch. Thus, b-1 is 0.10 inch high; b-2, 0.15 inch high; and b-3, 0.20 inch high. Pressure measurements were made at each ledge-height condition investigated, with all ledges downstream of ledge b removed to avoid the complication of interrelated effects.

The results of this investigation are shown in figure 13. Figure 13(a) is a plot of $\Delta \bar{h}_{1,2}/q_{c_1}$ as a function of inlet pressure ratio, with ledge heights as the parameters. A weight-flow check was made to determine whether erroneous values of $\Delta \bar{h}_{1,2}/q_{c_1}$ were obtained for these configurations, and as indicated by figure 13(c), no corrections to $\Delta \bar{h}_{1,2}/q_{c_1}$ were required.

The curves shown in figure 13(a) indicate that, in general, the height of smooth ledge b, over the range of heights investigated, does not appreciably influence the total-pressure performance of the diffuser. Although the values of $\Delta \bar{h}_{1,2}/q_{c_1}$ for the 0.20-inch ledge height (configuration b-3) are slightly lower than those for either of the other two ledge heights investigated, this occurrence is not considered significant in view of the static-pressure result shown in figure 13(b). Figure 13(b) demonstrates the variation of $\Delta p/\Delta p_{ideal}$ with inlet pressure ratio for the three ledge heights investigated, and it is evident that a single curve can be drawn through the data points for all configurations. The comparison curve of $\Delta p/\Delta p_{ideal}$ for the two 0.1-inch rough ledges (configuration b) is slightly higher than the single curve drawn for the

smooth ledges, although at higher speeds the difference in values of $\Delta p/\Delta p_{ideal}$ for the two types of ledges becomes nonexistent. In view of the static-pressure results, any apparent influence of the trailing-edge height of the smooth ledge on diffuser performance is suspect.

SUMMARY OF RESULTS

An experimental investigation was conducted to determine the effect of rough and smooth triangular ledges, approximately one-tenth of the inlet boundary-layer thickness in height, on the performance of a 23° conical diffuser with a 2:1 ratio of exit to inlet area and with a constant-area tailpipe about $3\frac{1}{2}$ inlet diameters in length. The inlet boundary-layer thickness was of the order of 5 percent of the inlet diameter. The air flows used in this investigation covered an inlet Mach number range from about 0.10 to 0.40, corresponding to Reynolds numbers from approximately 1×10^6 to 4×10^6 based on inlet diameter. The rough ledges consisted of graded cork particles and the smooth ledges of balsa-wood strips of triangular cross section. The following results were obtained:

1. The unstable flows in the diffuser were made stable by placing a 1-inch-wide strip of roughness just downstream of the inlet. Addition of more ledges had little or no effect on the stability of the flow in the diffuser although some evidence of flow asymmetry was noted for some configurations.

2. For the configurations investigated, the static-pressure recovery and the total-pressure-loss coefficient were either unaffected or slightly impaired by the installation of various arrangements of rough and smooth ledges.

Langley Aeronautical Laboratory,
National Advisory Committee for Aeronautics,
Langley Field, Va., September 11, 1953.

REFERENCES

1. Tillmann, W.: Investigations of Some Particularities of Turbulent Boundary Layers on Plates. Reps. and Translations No. 45, British M.A.P. Völkenrode, Mar. 15, 1946. (Issued by Joint Intelligence Objectives Agency with File No. B.I.G.S. - 19.)

2. Klebanoff, P. S., and Diehl, Z. W.: Some Features of Artificially Thickened Fully Developed Turbulent Boundary Layers With Zero Pressure Gradient. NACA TN 2475, 1951.

3. Newman, B. G.: The Re-Attachment of a Turbulent Boundary-Layer Behind a Spoiler. Rep. A. 64, Aero. Res. Lab. (Melbourne), Oct. 1949.

4. Persh, Jerome, and Bailey, Bruce M.: A Method for Estimating the Effect of Turbulent Velocity Fluctuations in the Boundary Layer on Diffuser Total-Pressure-Loss Measurements. NACA TN 3124, 1954.

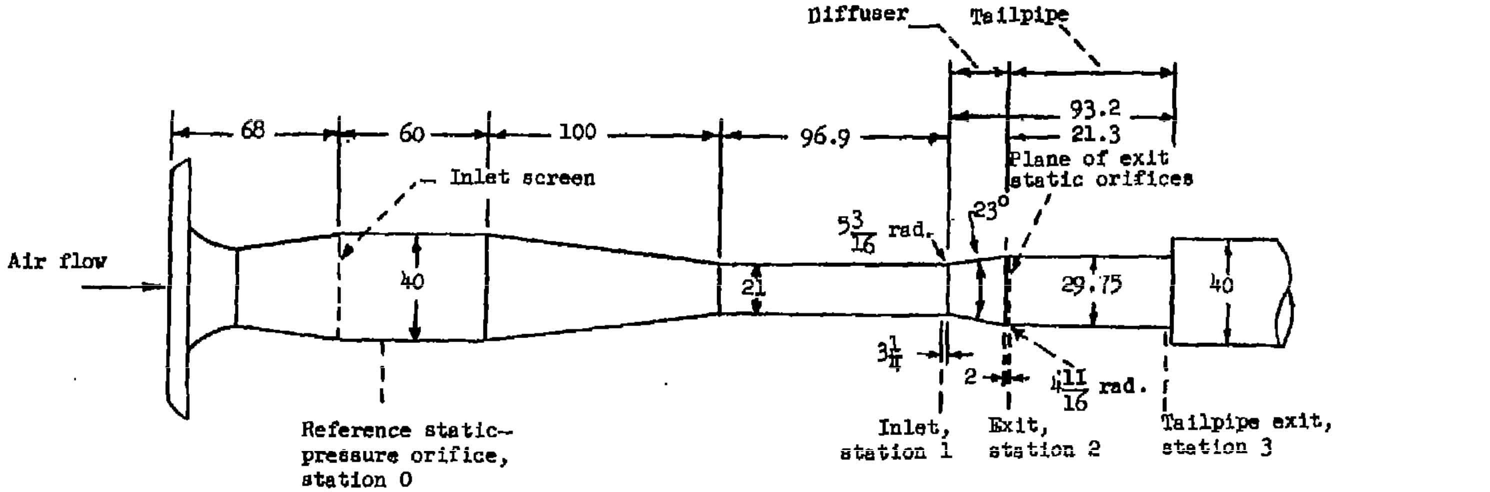

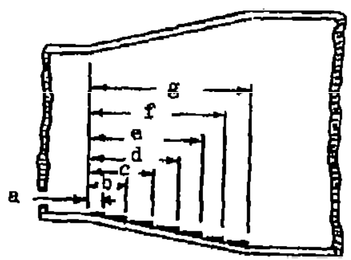

Cross section of diffuser showing longitudinal position of ledges

Configuration	Distance from inlet diffuser junction
a	1.49
b	5.00
c	8.40
d	11.72
e	15.14
f	18.21
g	21.30

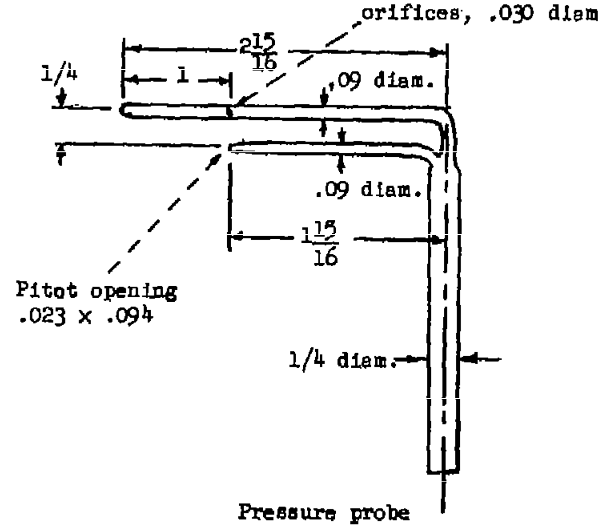

Pressure probe

Figure 1.- General arrangement of test apparatus and instrumentation. All dimensions are in inches.

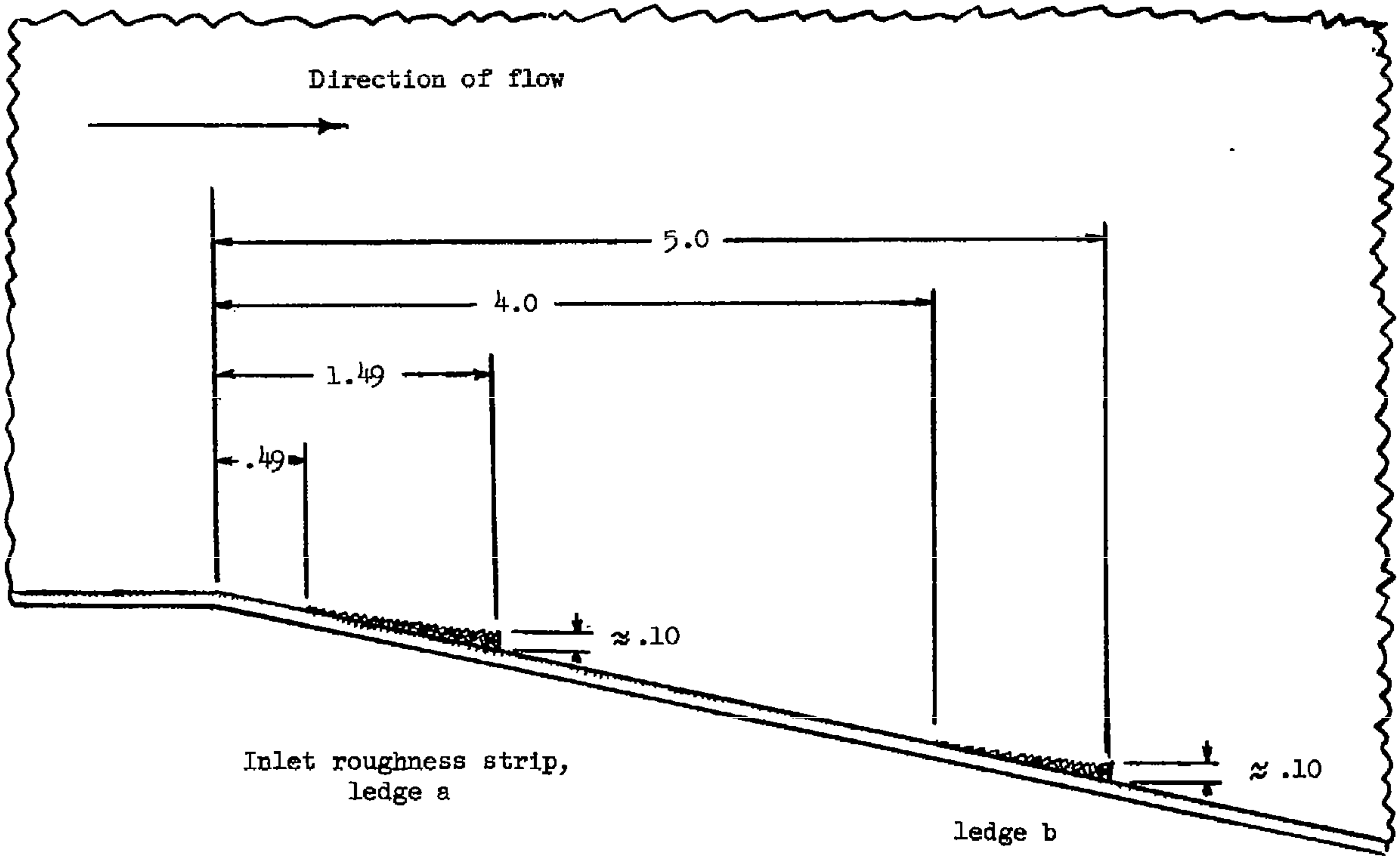

Figure 2.- Enlarged cross section of diffuser near inlet showing construction of inlet roughness strip, ledge a, and rough ledge b.

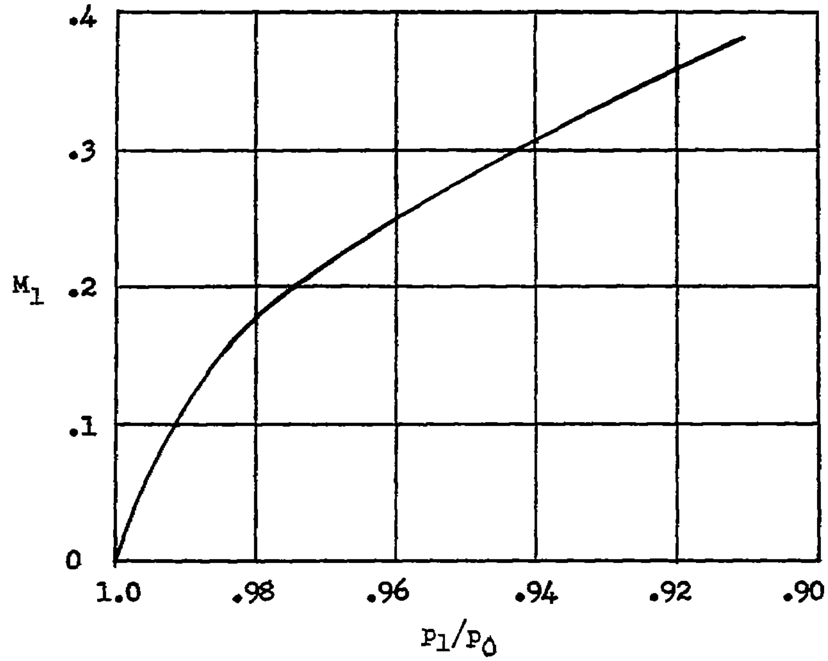

(a) Variation of inlet Mach number with inlet pressure ratio.

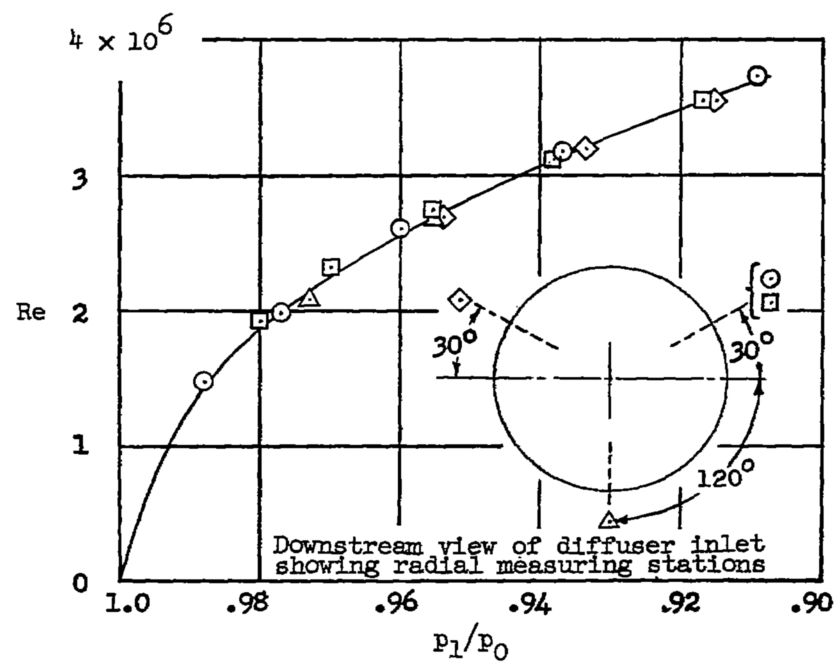

(b) Variation of inlet Reynolds number with inlet pressure ratio.

Figure 3.- Diffuser inlet conditions as functions of inlet pressure ratio.

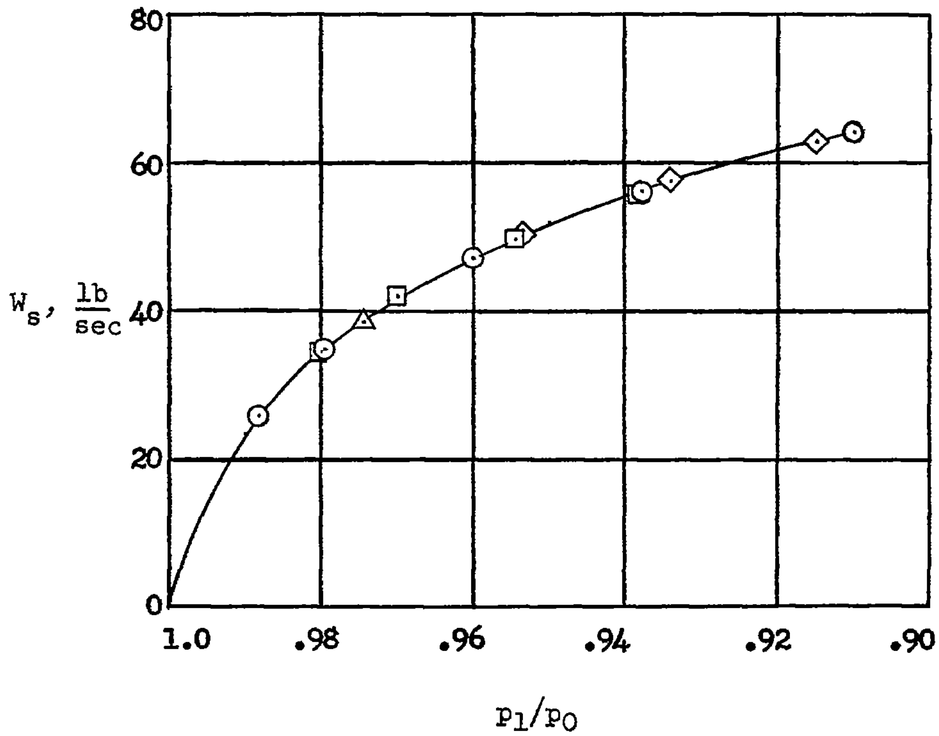

(c) Variation of standard weight flow at diffuser inlet with inlet pressure ratio. $W_s = \frac{29.92}{P}\sqrt{\frac{T}{520}}W_a$.

Figure 3.- Concluded.

$\frac{p_1}{p_0}$	δ^*, in.	θ, in.	H
0.9880	0.188	0.135	1.392
.9792	.175	.133	1.315
.9600	.163	.128	1.275
.9100	.144	.119	1.208

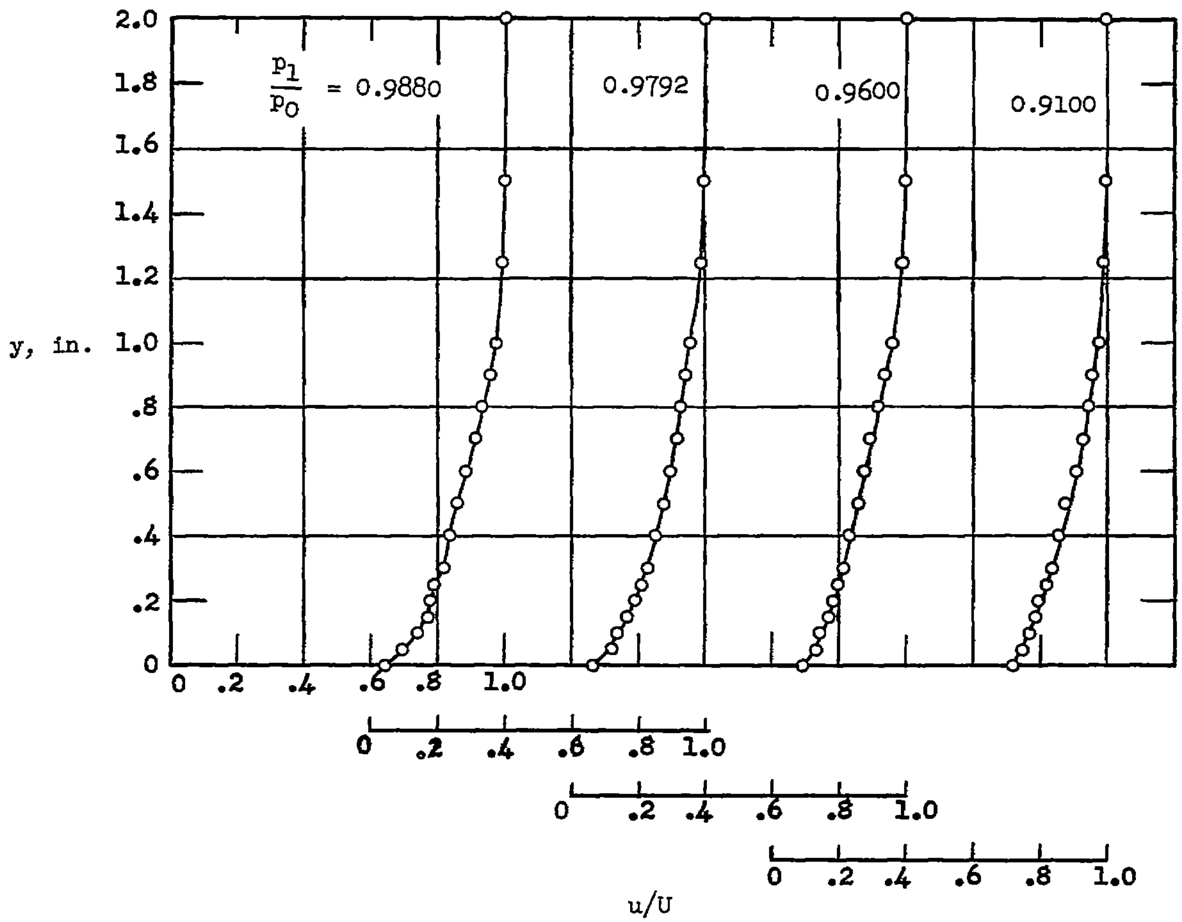

Figure 4.- Typical inlet velocity profiles at several values of inlet pressure ratio (station 1).

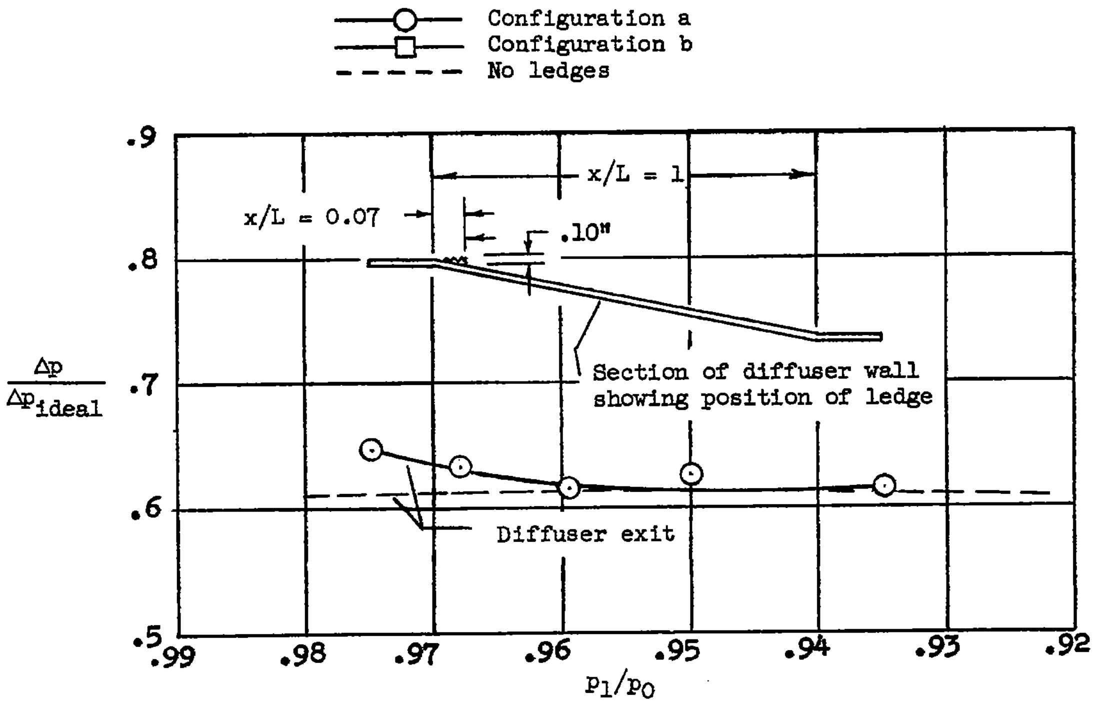

(a) Configuration a.

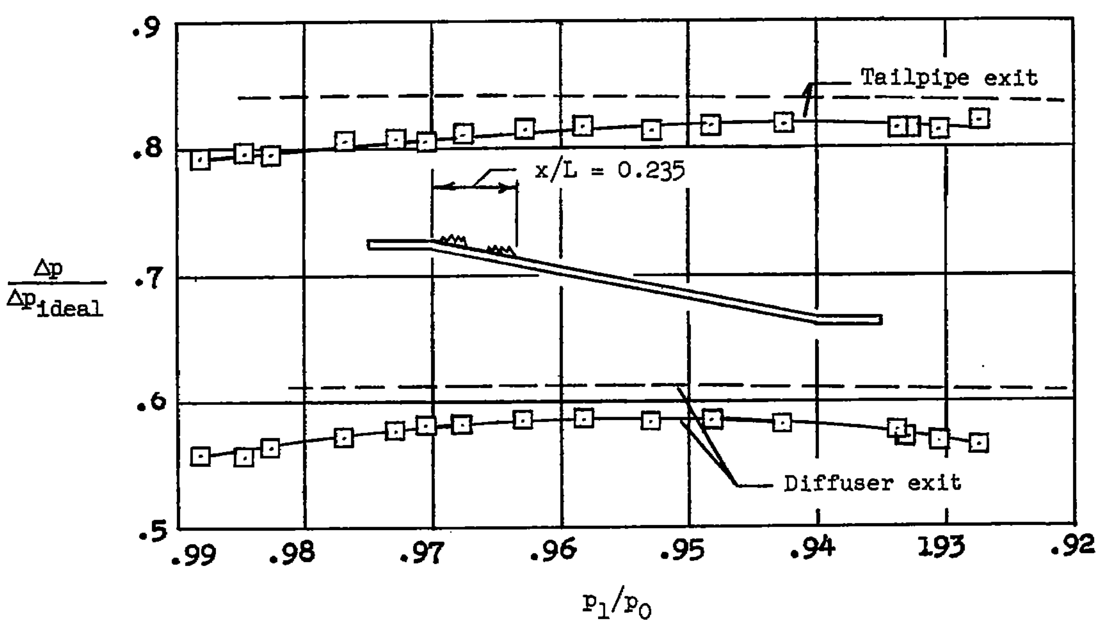

(b) Configuration b.

Figure 5.- Variation of diffuser effectiveness with inlet pressure ratio for configurations a, b, c, d, e, f, and g.

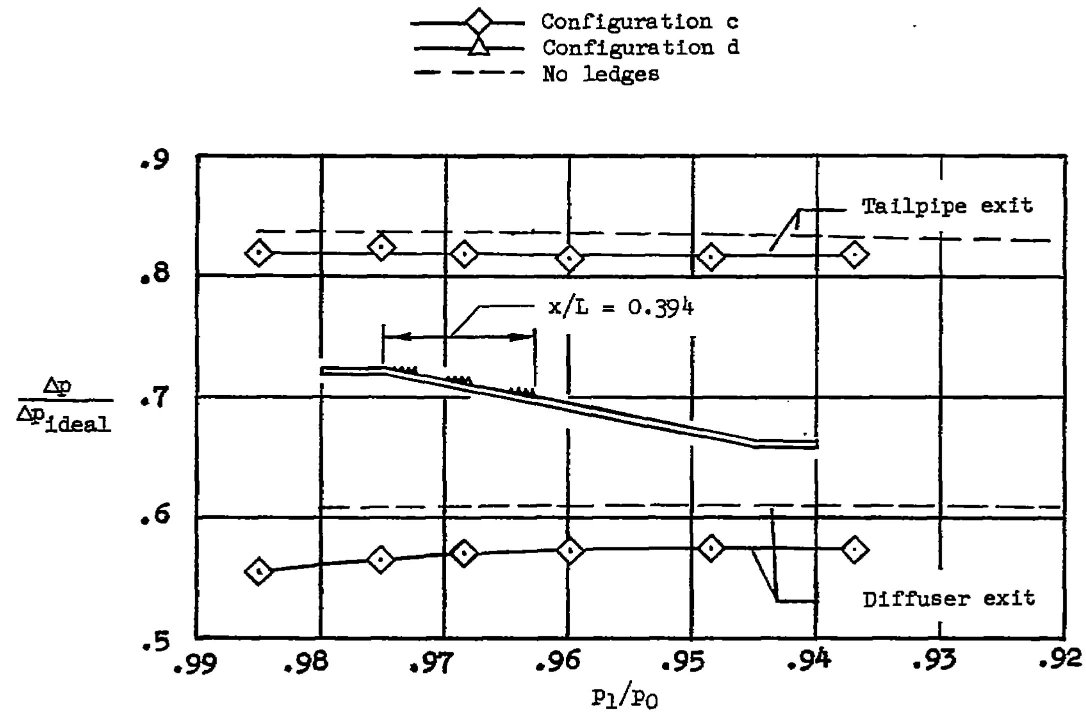

(c) Configuration c.

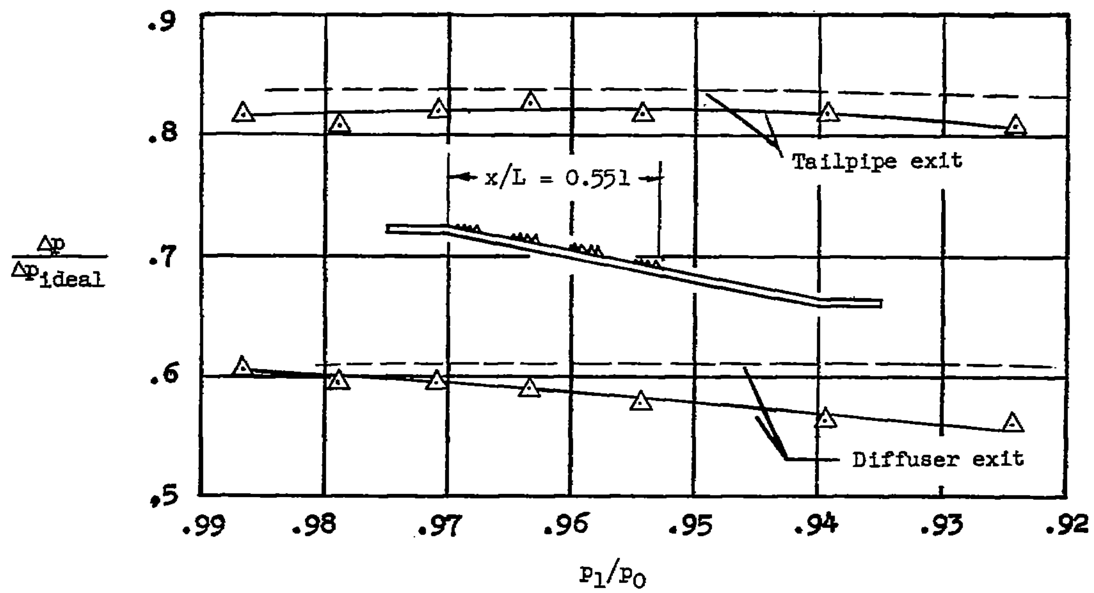

(d) Configuration d.

Figure 5.- Continued.

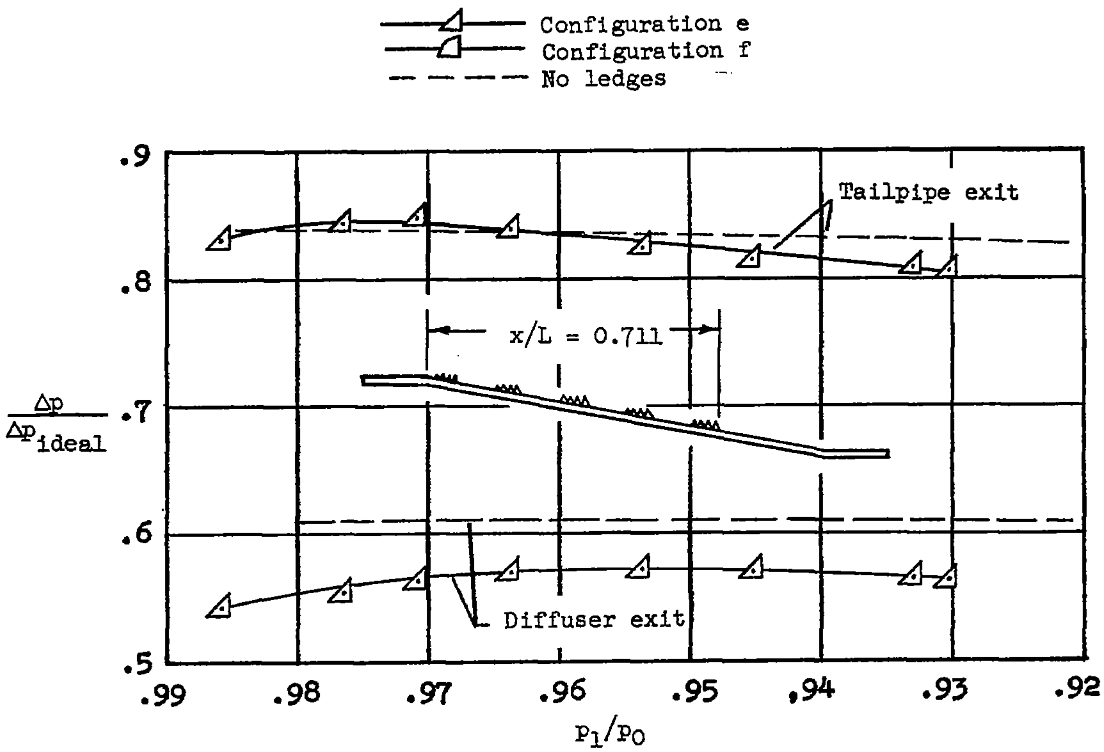

(e) Configuration e.

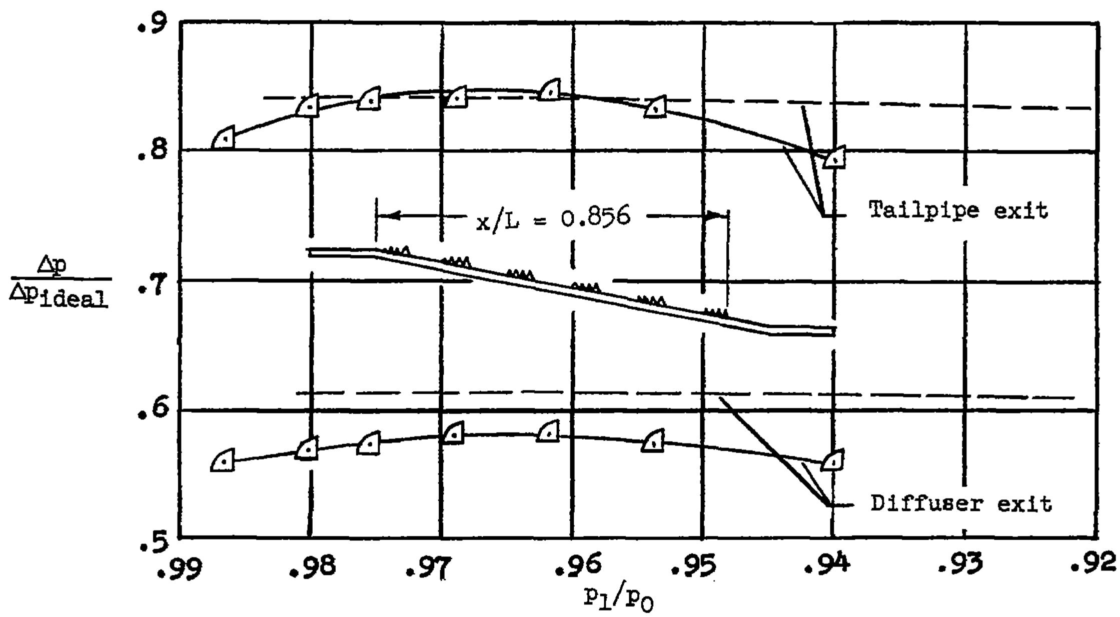

(f) Configuration f.

Figure 5.- Continued.

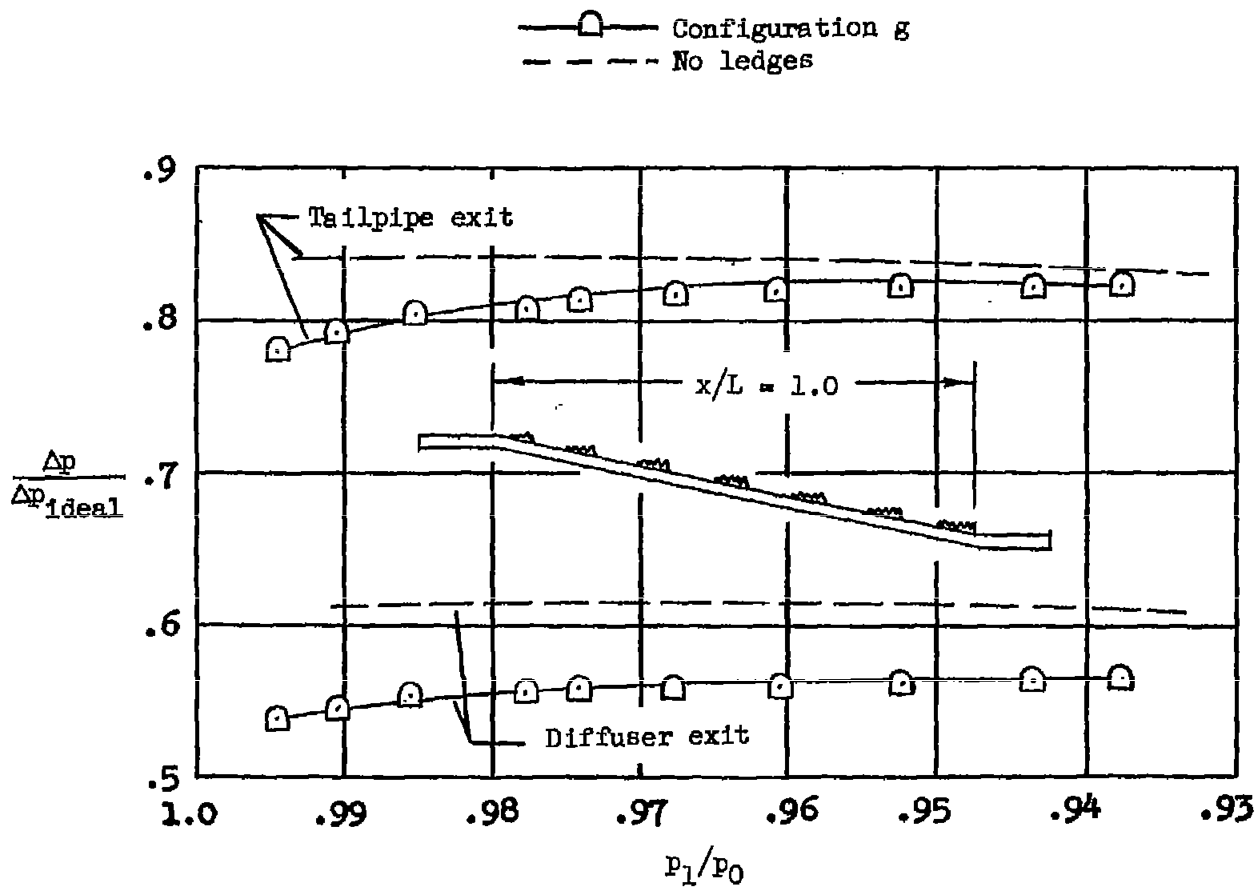

(g) Configuration g.

Figure 5.- Concluded.

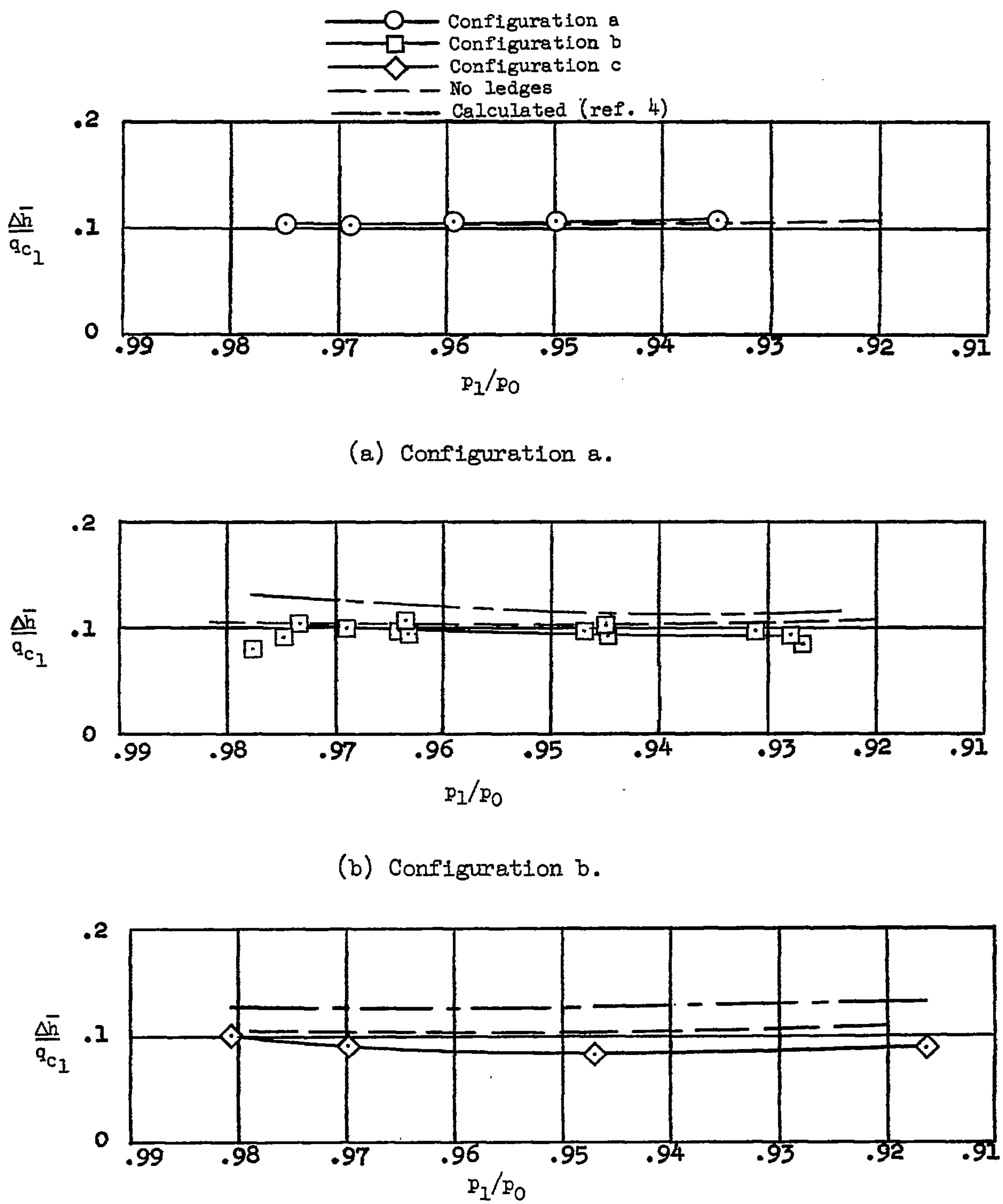

(a) Configuration a.

(b) Configuration b.

(c) Configuration c.

Figure 6.- Variation of total-pressure-loss coefficient with inlet pressure ratio for configurations a, b, c, d, f, and g.

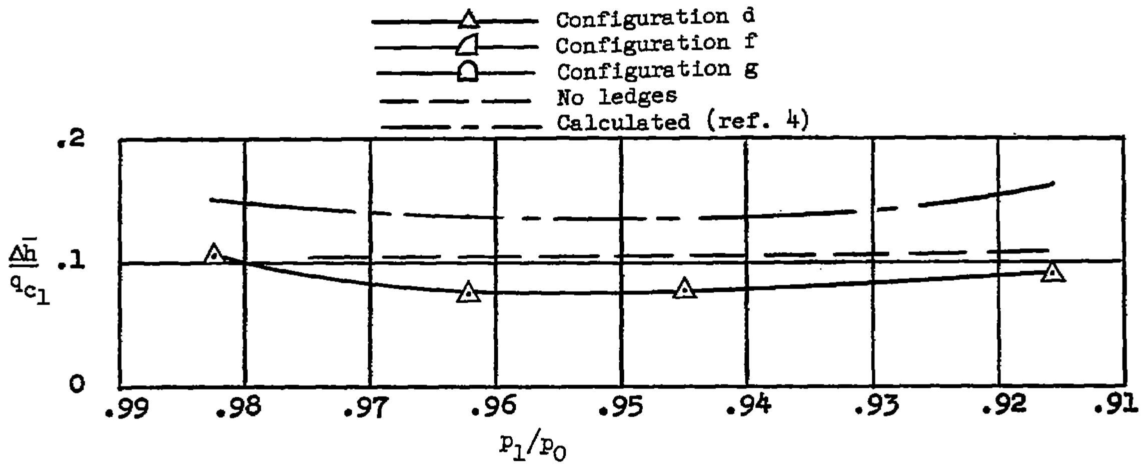

(d) Configuration d.

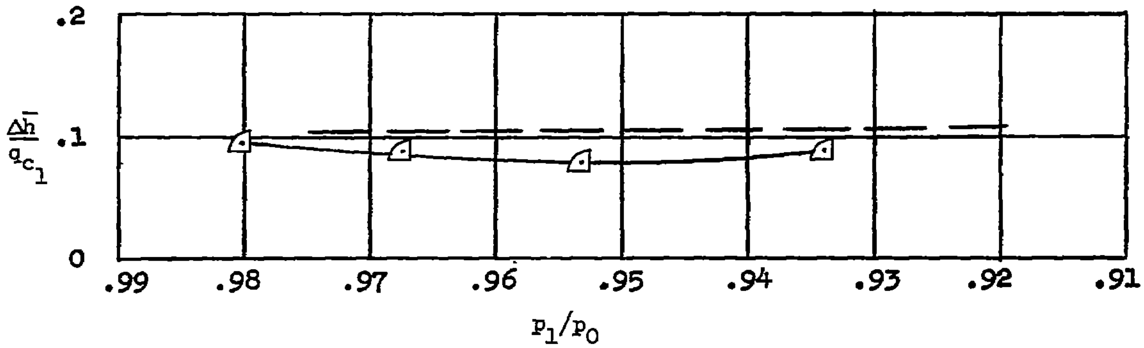

(e) Configuration f.

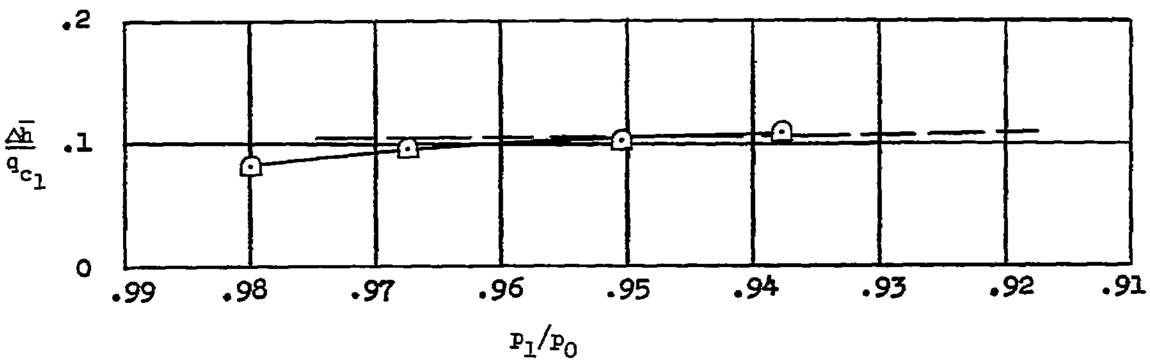

(f) Configuration g.

Figure 6.- Concluded.

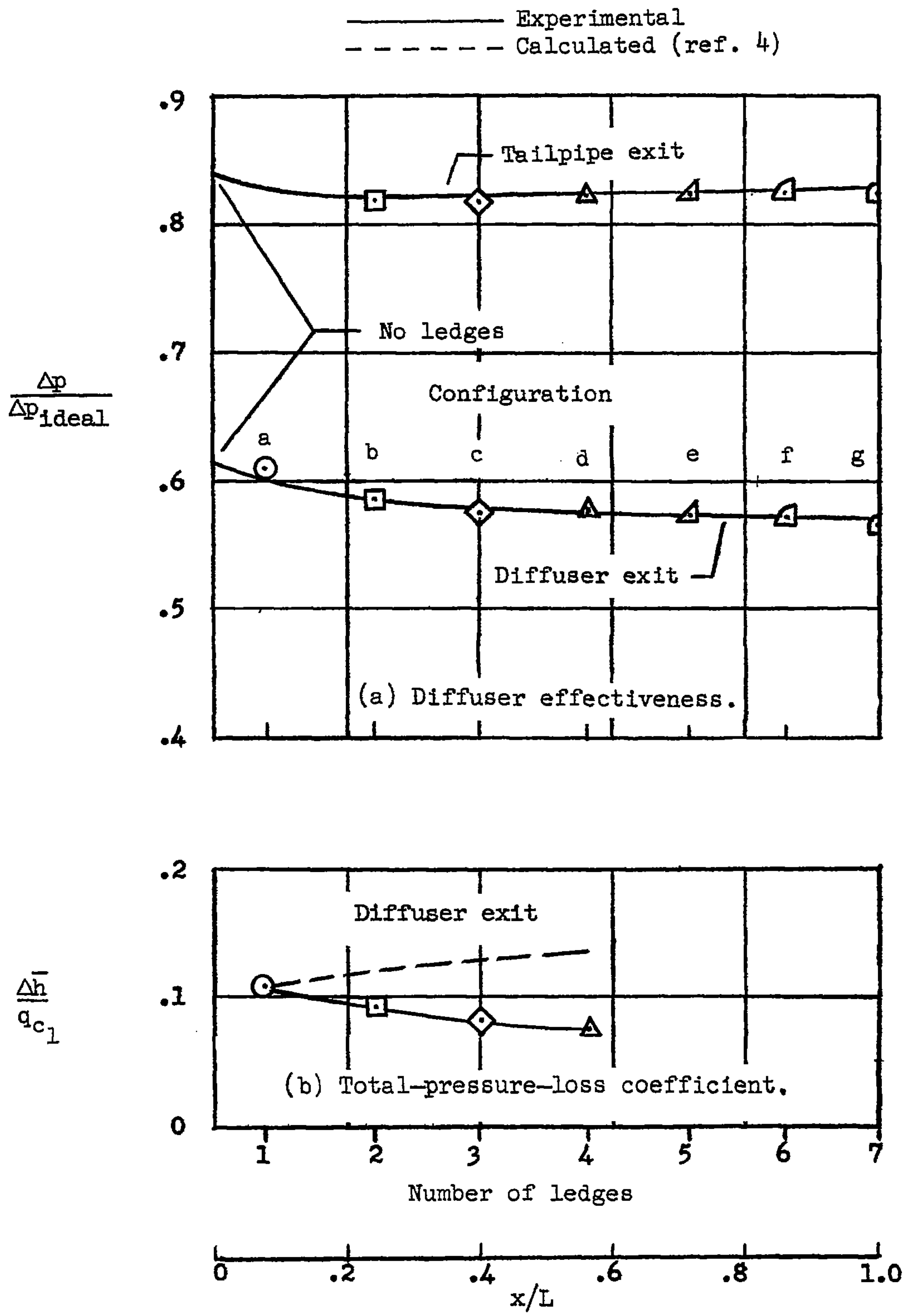

Figure 7.- Variation of diffuser performance parameters with x/L at constant inlet pressure ratio of 0.95 for configurations a, b, c, d, e, f, and g.

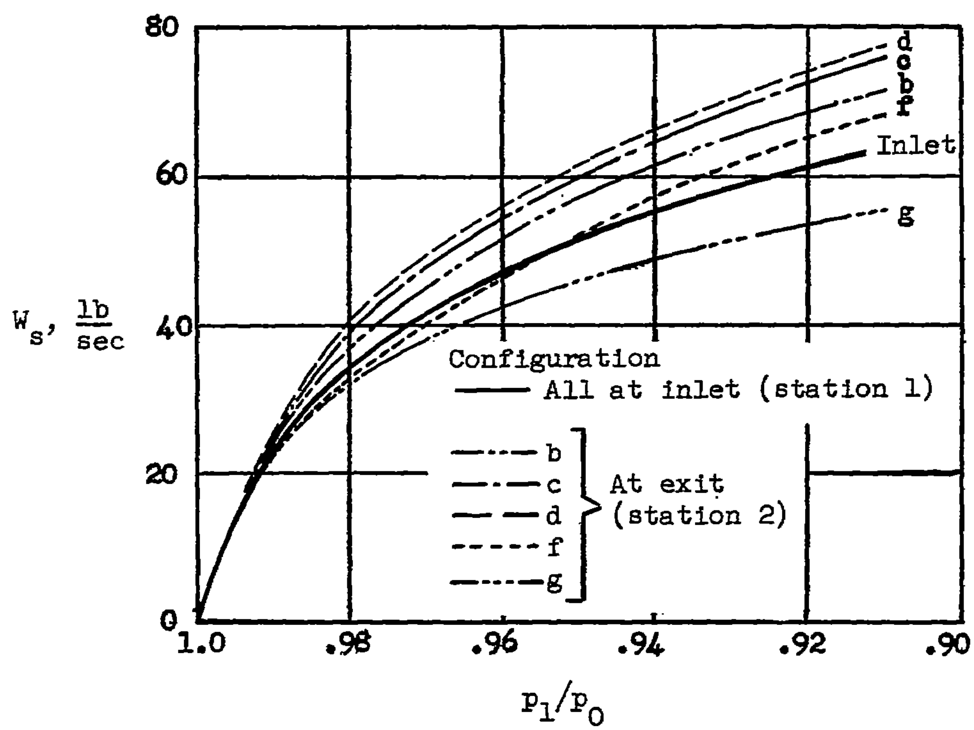

Figure 8.- Comparison between standard inlet weight flows and standard exit weight flows for configurations b, c, d, f, and g.

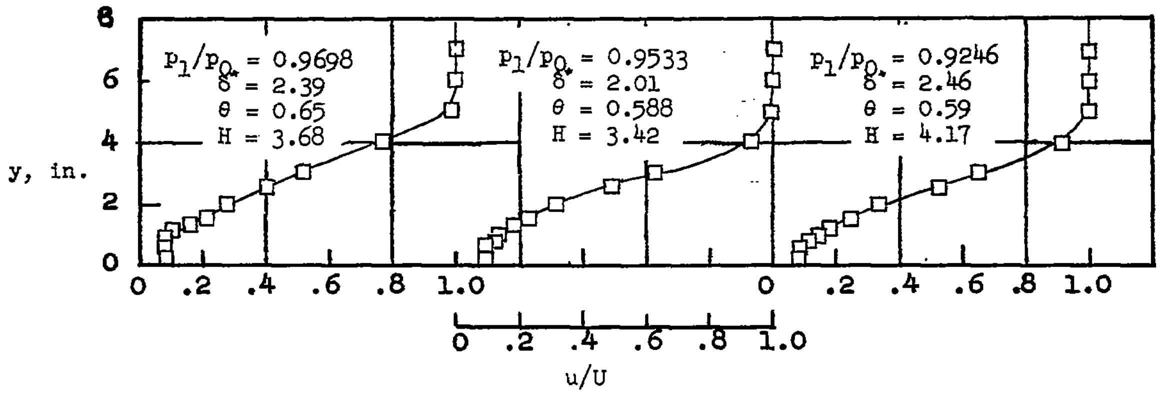

(a) Configuration b.

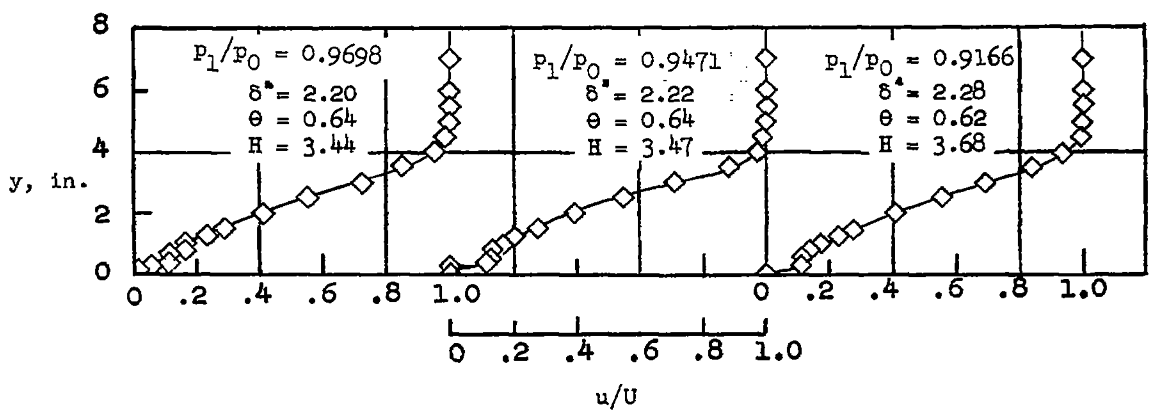

(b) Configuration c.

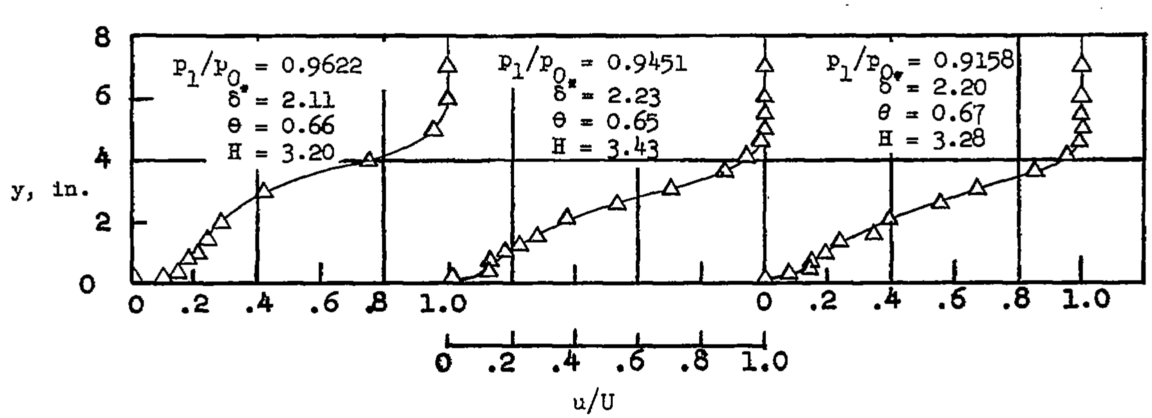

(c) Configuration d.

Figure 9.- Boundary-layer velocity profiles at diffuser exit (station 2) for configurations b, c, d, f, and g.

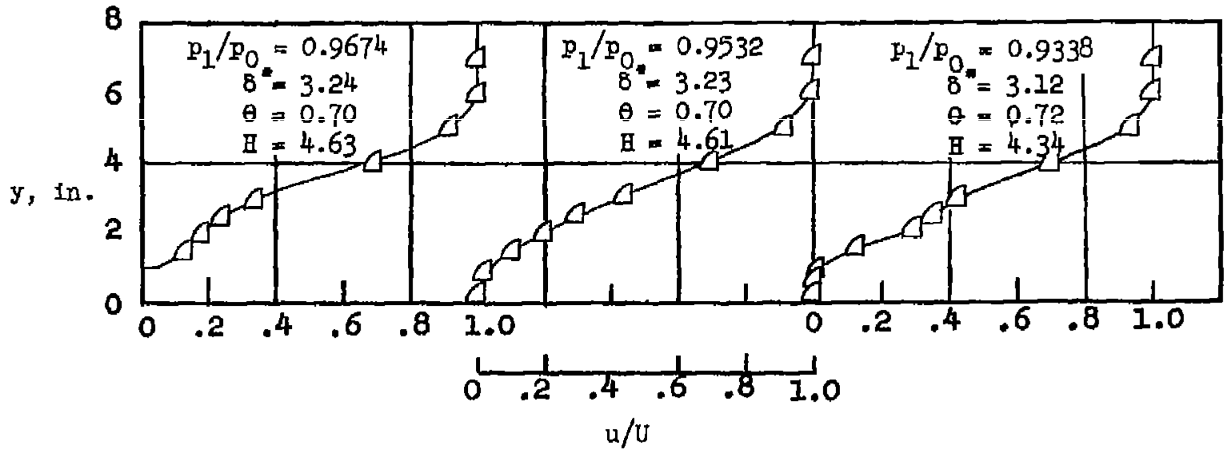

(d) Configuration f.

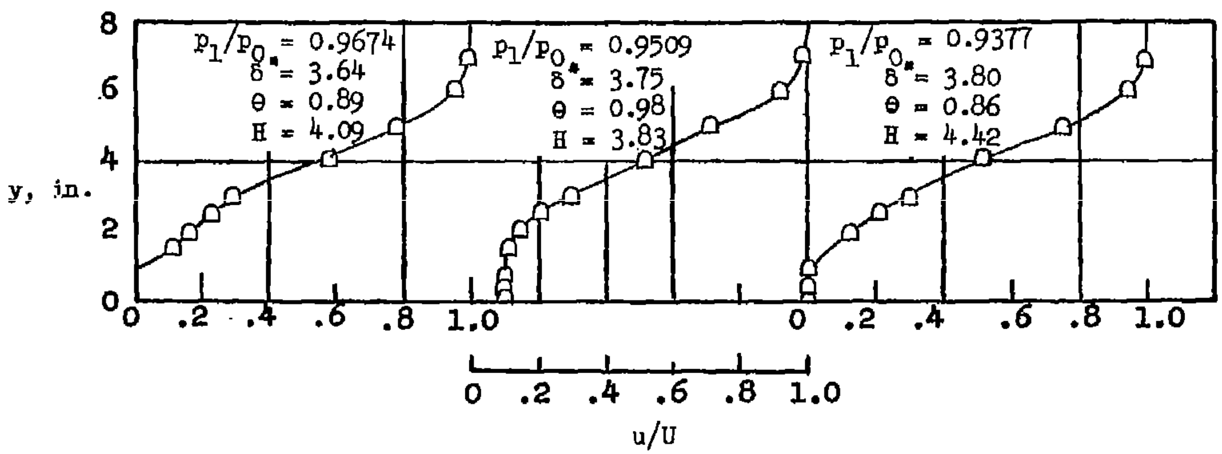

(e) Configuration g.

Figure 9.- Concluded.

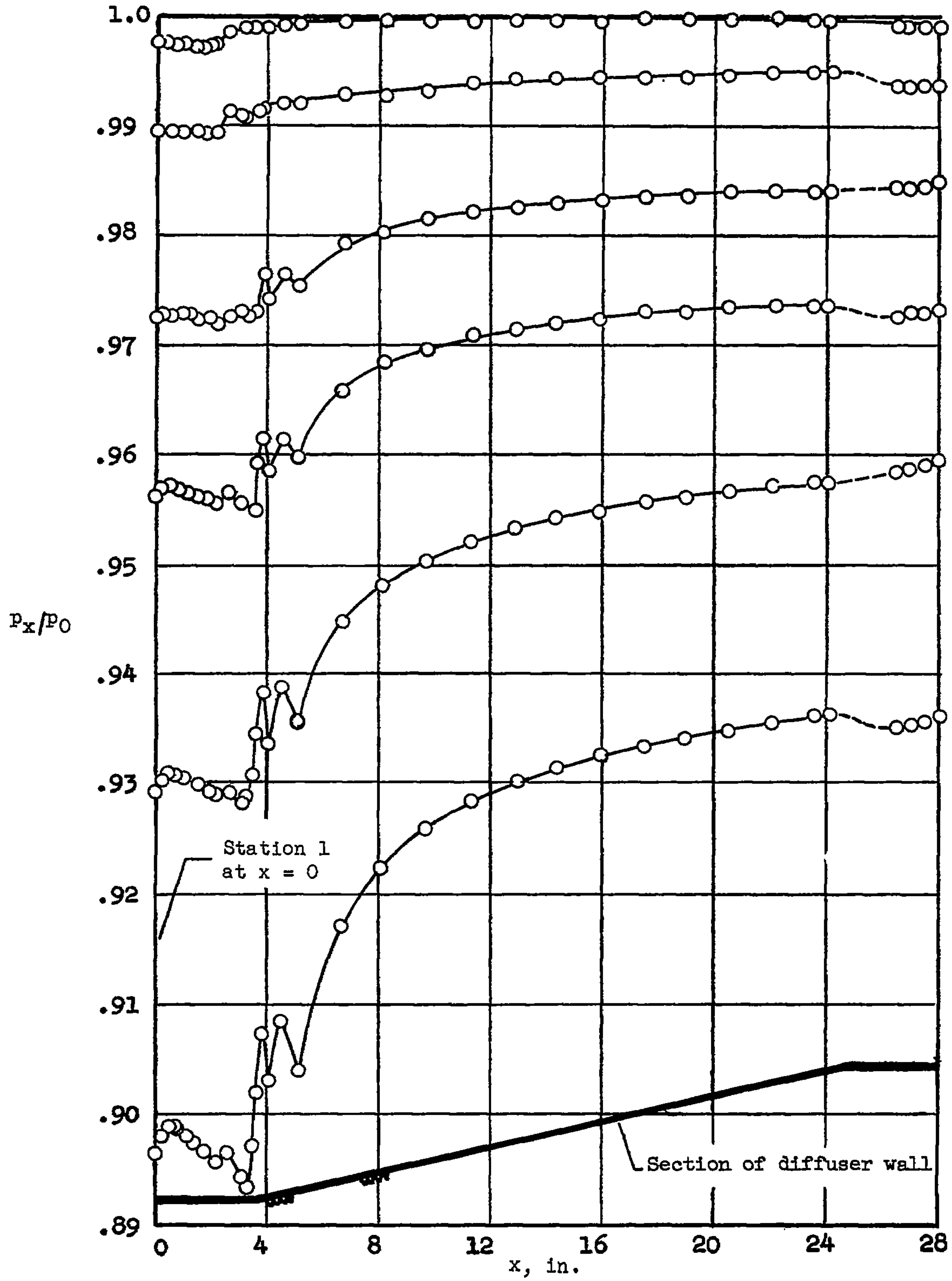

Figure 10.- Variation of static-pressure distribution along length of diffuser (configuration b).

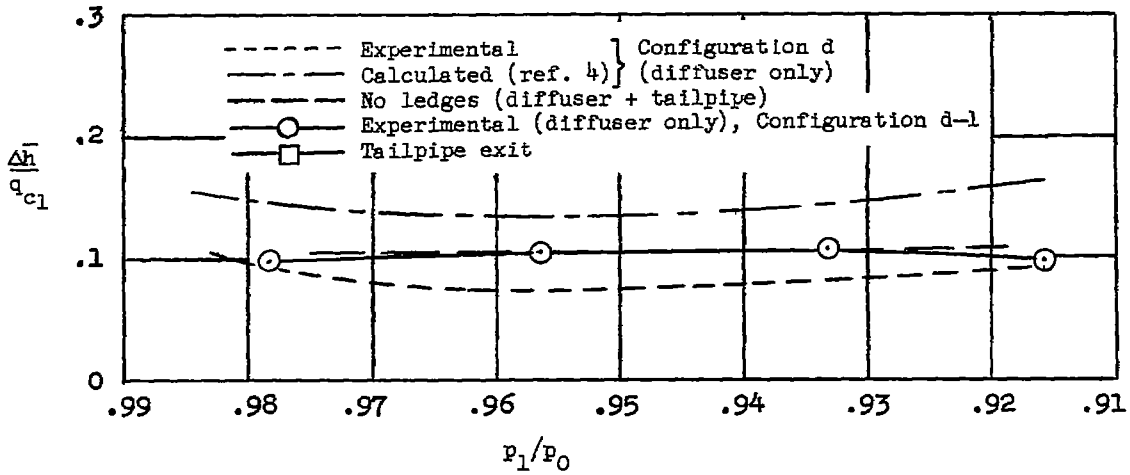

(a) Total-pressure-loss coefficient.

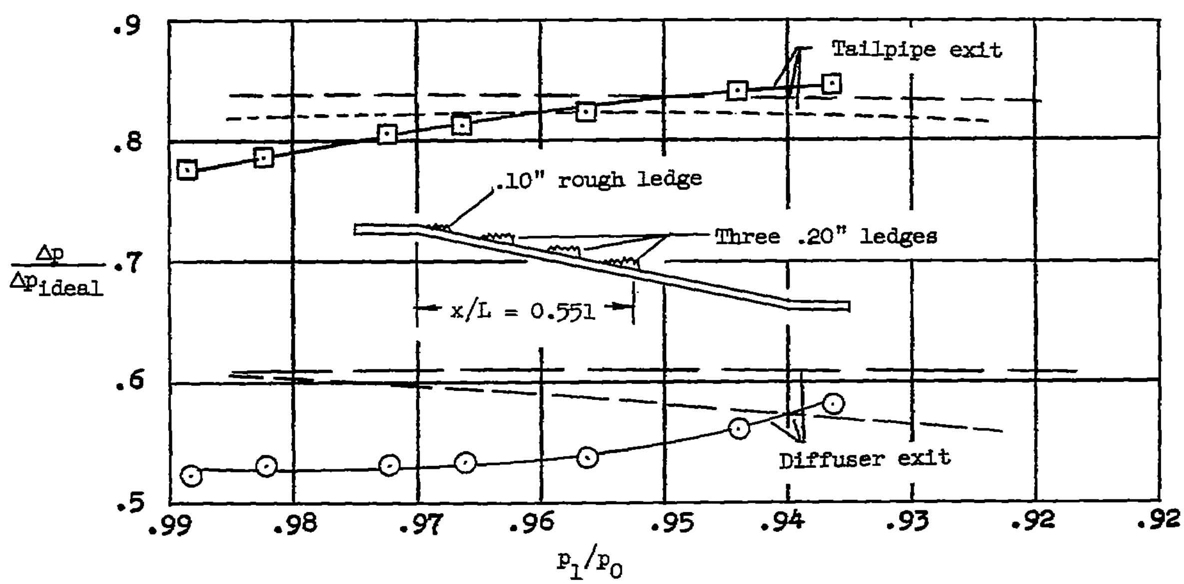

(b) Diffuser effectiveness.

Figure 11.- Variation of diffuser performance parameters with inlet pressure ratio (configuration d-1).

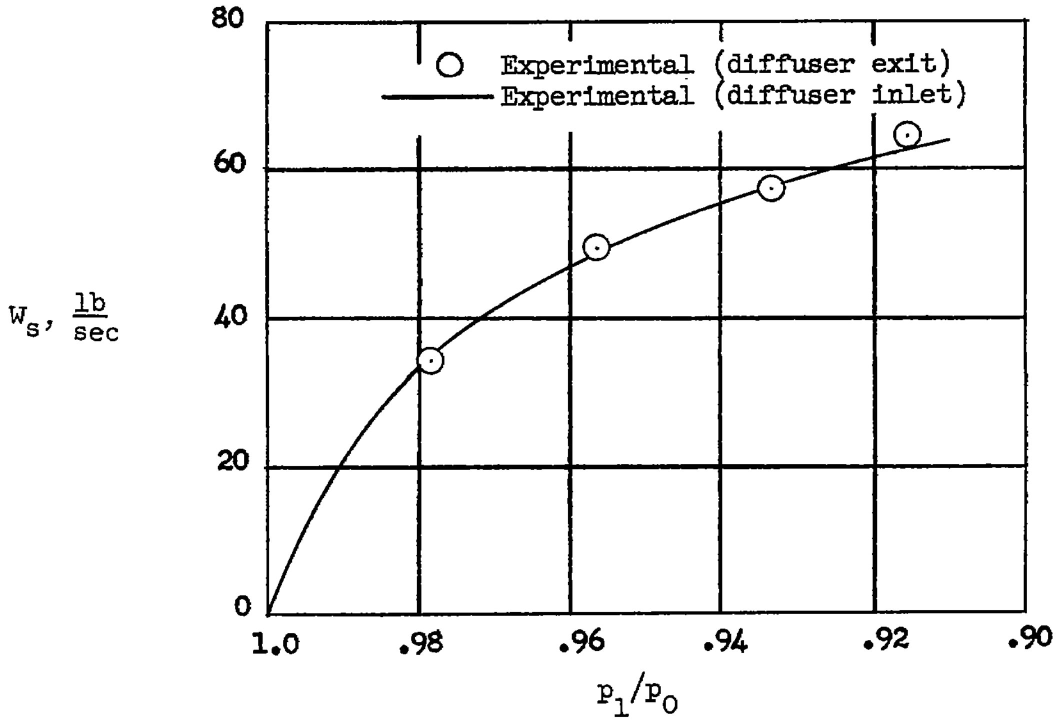

(c) Variation of standard weight flow with inlet pressure ratio.

Figure 11.- Concluded.

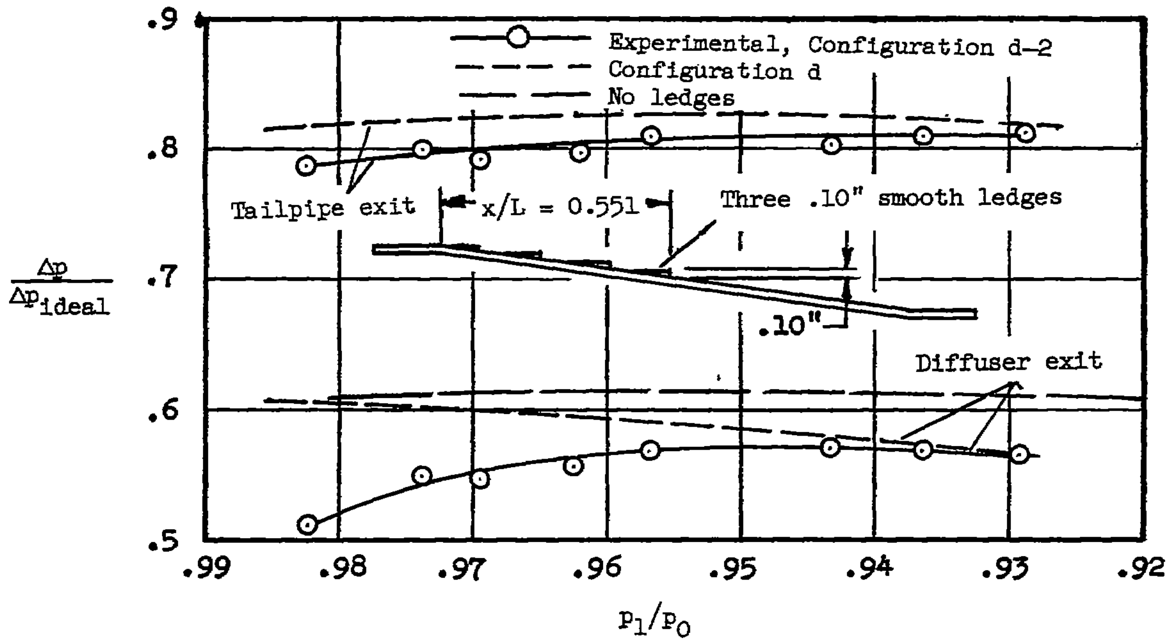

(a) Diffuser effectiveness.

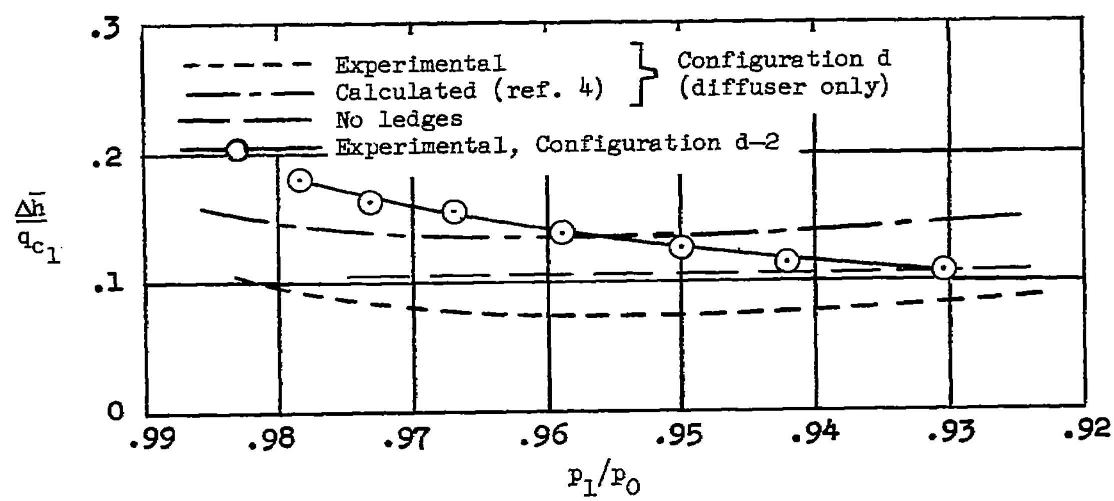

(b) Total-pressure-loss coefficient.

Figure 12.- Variation of diffuser performance parameters with inlet pressure ratio for configuration d-2.

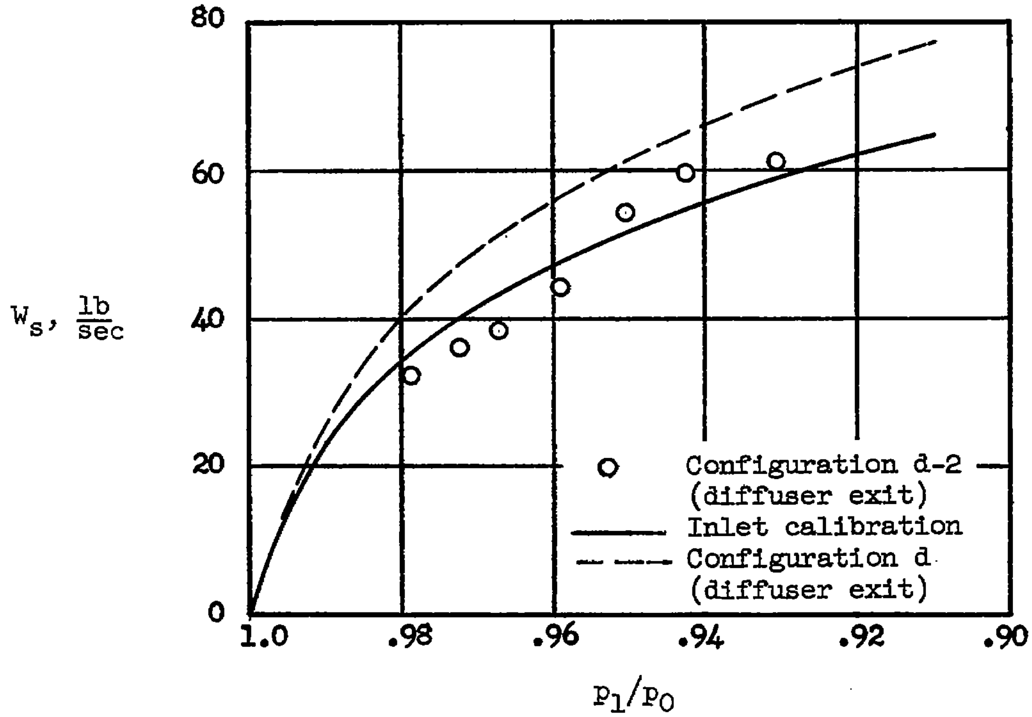

(c) Variation of standard weight flow with inlet pressure ratio.

Figure 12.- Concluded.

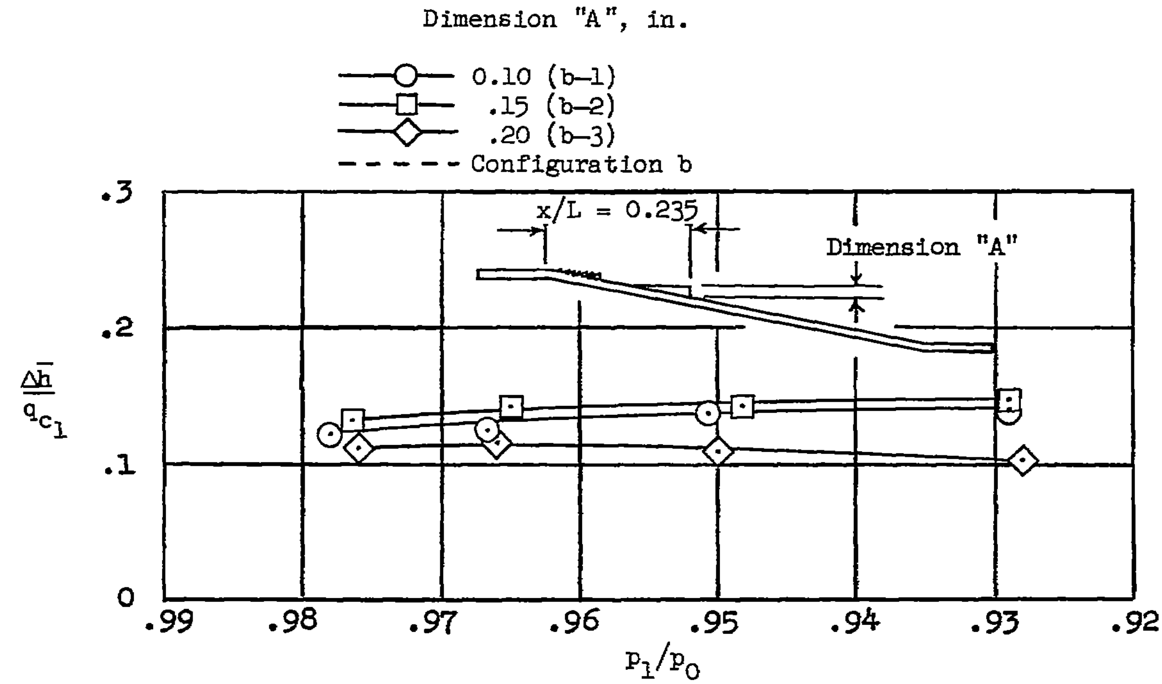

(a) Total-pressure-loss coefficient.

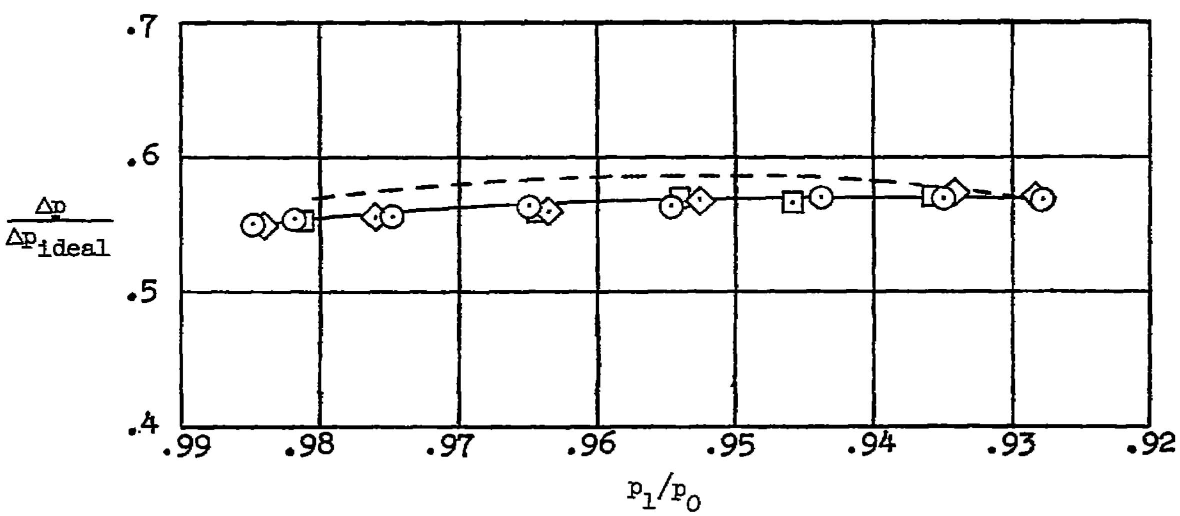

(b) Diffuser effectiveness.

Figure 13.- Variation of diffuser performance parameters with inlet pressure ratio for configurations b-1, b-2, and b-3.

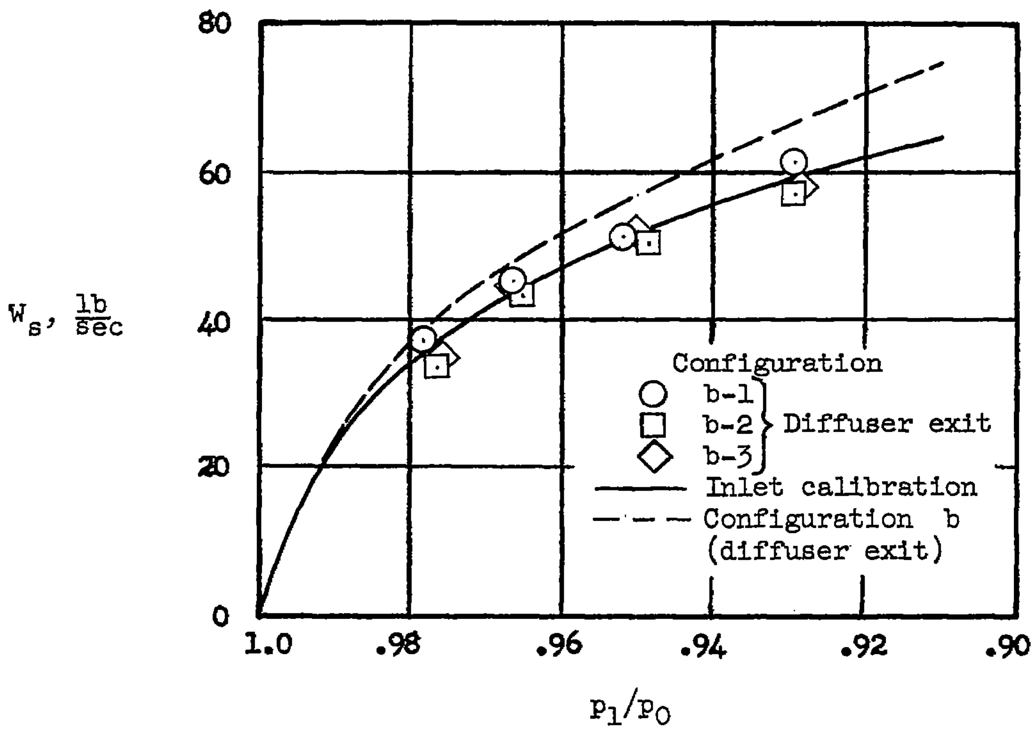

(c) Variation of standard weight flow with inlet pressure ratio.

Figure 13.- Concluded.

NACA-Langley - 1-29-54 - 1000